that do not interact with the CP/T at this stage are variable in shape, while binding to cargo restricts their freedom of movement (*14*). The contour line view reveals that the narrowest constriction of the central channel is situated at the cytoplasmic side of the lumenal spoke ring in the CF class, even though it is at the nuclear side of the same ring in the LR class (Fig. 4B). These observations indicate that major rearrangements in the spokes might play a critical role in the translocation of cargo.

Both classes represent major structural states of the NPC. Since the CP/T is better defined in the CF class, this state might represent the slow incorporation or release of cargo complexes into or from the FXFG-framework residing in the central channel (*15*), which involves interaction with the cytoplasmic filaments. The more diffuse CP/T of the LR class indicates that cargo complexes can be found in various positions once they have entered the channel [in agreement with (*16*)]. Although an assignment of the classes to import, export or to predominant rate-limiting steps in both processes is not yet possible, the application of cryo-ET to transport-competent, intact nuclei holds great potential for a structural dissection of the key steps involved. The use of defined cargo and the trapping of distinct transport intermediates should ultimately enable us to arrive at a detailed mechanistic understanding of the nuclear pore complex.

References and Notes

1. M. Suntharalingam, S. R. Wente, *Dev. Cell* **4**, 775 (2003).
2. D. Stoffler *et al.*, *J. Mol. Biol.* **328**, 119 (2003).
3. W. Baumeister, *Curr. Opin. Struct. Biol.* **12**, 679 (2002).
4. O. Medalia *et al.*, *Science* **298**, 1209 (2002).
5. F. Melchior, B. Paschal, J. Evans, L. Gerace, *J. Cell Biol.* **123**, 1649 (1993).
6. Because the NPCs of spread *Xenopus* nuclear envelopes have a preferred orientation (*17*), an isotropically resolved structure cannot be obtained from such samples (although transport active), owing to the missing cone problem (*11*).
7. M. W. Goldberg, T. D. Allen, *J. Mol. Biol.* **257**, 848 (1996).
8. E. Kiseleva *et al.*, *J. Struct. Biol.* **145**, 272 (2004).
9. Q. Yang, M. P. Rout, C. W. Akey, *Mol. Cell* **1**, 223 (1998).
10. C. W. Akey, M. Radermacher, *J. Cell Biol.* **122**, 1 (1993).
11. K. Grunewald, O. Medalia, A. Gross, A. C. Steven, W. Baumeister, *Biophys. Chem.* **100**, 577 (2003).
12. M. P. Rout *et al.*, *J. Cell Biol.* **148**, 635 (2000).
13. E. Kiseleva, M. W. Goldberg, T. D. Allen, C. W. Akey, *J. Cell Sci.* **111**, 223 (1998).
14. N. Pante, U. Aebi, *Science* **273**, 1729 (1996).
15. B. Fahrenkrog, U. Aebi, *Nat. Rev. Mol. Cell Biol.* **4**, 757 (2003).
16. W. Yang, J. Gelles, S. M. Musser, *Proc. Natl. Acad. Sci. U.S.A.* **101**, 12887 (2004).
17. J. P. Siebrasse, R. Peters, *EMBO Rep.* **3**, 887 (2002).

18. We thank R. Hegerl for help with the image processing and A. Leis, V. Lucic, and P. Zwickl for critical reading of the manuscript.

Supporting Online Material
www.sciencemag.org/cgi/content/full/1104808/DC1
Materials and Methods
Figs. S1 to S3
References and Notes

3 September 2004; accepted 24 September 2004
Published online 28 October 2004;
10.1126/science.1104808
Include this information when citing this paper.

Anabaena Sensory Rhodopsin: A Photochromic Color Sensor at 2.0 Å

Lutz Vogeley,[1] Oleg A. Sineshchekov,[3,5] Vishwa D. Trivedi,[3] Jun Sasaki,[3] John L. Spudich,[3,4]* Hartmut Luecke[1,2]*

Microbial sensory rhodopsins are a family of membrane-embedded photoreceptors in prokaryotic and eukaryotic organisms. Structures of archaeal rhodopsins, which function as light-driven ion pumps or photosensors, have been reported. We present the structure of a eubacterial rhodopsin, which differs from those of previously characterized archaeal rhodopsins in its chromophore and cytoplasmic-side portions. *Anabaena* sensory rhodopsin exhibits light-induced interconversion between stable 13-cis and all-trans states of the retinylidene protein. The ratio of its cis and trans chromophore forms depends on the wavelength of illumination, thus providing a mechanism for a single protein to signal the color of light, for example, to regulate color-sensitive processes such as chromatic adaptation in photosynthesis. Its cytoplasmic half channel, highly hydrophobic in the archaeal rhodopsins, contains numerous hydrophilic residues networked by water molecules, providing a connection from the photoactive site to the cytoplasmic surface believed to interact with the receptor's soluble 14-kilodalton transducer.

Over the past 4 years, microbial genomics has revealed a large family of photoactive, seven-transmembrane-helix retinylidene proteins called microbial rhodopsins in phylogenetically diverse species, including haloarchaea, proteobacteria, cyanobacteria, fungi, and algae (*1*–*4*). The first members of this family were discovered in halophilic archaea: the light-driven ion pumps bacteriorhodopsin and halorhodopsin and the phototaxis receptors sensory rhodopsins I and II. These four related haloarchaeal pigments are among the best-characterized membrane proteins in terms of structure and function, and nearly all of our knowledge of the properties of microbial rhodopsins, such as isomeric configuration and conformation of their chromophore, photochemical reactions, light-induced conformational changes in the protein, and function, derives from the study of these four, including atomic resolution structures that have been obtained for three of them (*5*–*9*). Studies of non-haloarchaeal rhodopsins, of which >800 are known to exist (*10*, *11*), are needed to examine the diversity of properties of this widespread family (*12*). *Anabaena* sensory rhodopsin, a recently discovered sensory representative outside of archaea (*2*), is well suited for exploration. It is the only bacterial sensory rhodopsin so far expressed in a photoactive form. Unlike the haloarchaeal sensory rhodopsins, which transmit signals to other integral membrane proteins, its function appears to involve modulation of a soluble cytoplasmic transducer, analogous to animal visual pigments (*2*).

In this study, we report the structure of the retinal-complexed protein at 2.0 Å resolution, obtained by X-ray diffraction of crystals grown in a cubic lipid phase (table S1). The overall membrane-embedded seven-helical structure is similar to those of the archaeal rhodopsins. However, distinct differences in the photoactive site prompted analysis of the isomeric configuration of the retinal and the photochemical reactions of the pigment.

Despite intense white-light illumination [light adaptation (*13*)] of the crystals before cryocooling and X-ray data collection, which results in a fully all-trans retinal configuration in bacteriorhodopsin, maps of the retinal and Schiff base region of *Anabaena* sensory rhodopsin show electron density incompati-

[1]Department of Molecular Biology and Biochemistry, [2]Department of Physiology and Biophysics and Department of Informatics and Computer Sciences, University of California, Irvine, CA 92697, USA. [3]Center for Membrane Biology, Department of Biochemistry and Molecular Biology, [4]Department of Microbiology and Molecular Genetics, University of Texas Medical School, Houston, TX 77030, USA. [5]Biology Department, Moscow State University, Moscow, Russia.

*To whom correspondence should be addressed. E-mail: hudel@uci.edu (H.L.) or john.l.spudich@uth.tmc.edu (J.L.S.)

ble with 100% all-trans retinal (Fig. 1A). Subsequent extractions and chemical structure determinations of retinal isomers from orange-illuminated (580-nm) and blue-illuminated (480-nm) *Anabaena* pigment showed light-induced shifts of the isomeric configuration. In the fully dark-adapted state, the all-trans form [absorption maximum (λ_{max}) of 549 nm in detergent-solubilized membranes] predominates [>75%, (Fig. 1B)]. Orange illumination rapidly shifted the pigment to a stable >80% 13-cis state (λ_{max} of 537 nm), and blue light rapidly increased the all-trans content toward the dark-adapted isomer ratio (Fig. 1B). Therefore, the relative amounts of *Anabaena* sensory rhodopsin with cis and trans chromophore configurations depend on the quality (color) of illumination and are shifted between the two forms by pulses of orange and blue illumination (Fig. 1C). This photochromic property provides a possible mechanism for single-pigment color sensing. Its two distinct groundstate species thermally interconvert with halftimes of ~100 min and ~300 min for the trans and cis forms, respectively; this is a fundamental difference from that of another color-sensitive microbial rhodopsin, the archaeal phototaxis receptor sensory rhodopsin I (*14*). Such relatively long-lasting color sensitivity is similar to that of the red/far-red photochromic states of phytochrome and may be used, in the *Anabaena* cell in analogy to phytochrome (*15*–*17*), to control expression of proteins required under either orange-light or blue-light illumination. The photochromic reactions are also similar to those between 11-cis and all-trans forms of invertebrate visual pigments, which have been suggested to reset the 11-cis state in a light-dependent manner (*18*).

Further detailed structural analysis of the active site revealed two alternate conformations for Lys^{210}. In one, its carbonyl oxygen forms a regular α-helical hydrogen bond with the peptide of Ser^{214}; in the other, its hydrogen bond donor is a nearby water (Wat^{502}) (Fig. 2B). Wat^{502} also connects helices B and G by bridging the hydroxyl of Ser^{214} with the backbone carbonyl of Ala^{40}. Multiple conformations of the residue-210 peptide may be facilitated by the presence of a π bulge at residues Ser^{209}, Lys^{210}, and Val^{211}, which is believed to soften the otherwise relatively rigid α helix (*5*, *19*). A further reduction of the α-helical character of this region stems from the replacement of the aspartic residue at position 206 (anionic Asp^{212}, which is part of the complex counterion in bacteriorhodopsin), highly conserved in archaeal rhodopsins, with a proline, Pro^{206} (Fig. 2A). Although the α helix on both sides of Pro^{206} is undisturbed by the loss of the peptide amide of the proline, the main-chain carbonyl of residue 202 accepts a hydrogen bond from the hydroxyl of reoriented Tyr^{51}. In other microbial rhodopsin structures, the Tyr^{51} hydroxyl forms a strong hydrogen bond with the anionic aspartate carboxyl. The rearrangement also results in a 1.3 Å movement of Wat^{402}, the water that bridges the protonated Schiff base and its counterion (*5*, *7*, *20*), toward the β-ionone ring of the retinal. Wat^{402} receives hydrogen bonds from the Schiff base (3.0 Å versus 2.6 Å in sensory rhodopsin II) and from the Trp^{76} indole while donating hydrogen bonds to the OD2 of Asp^{75} and, weakly, to the hydroxyl of Tyr^{51}. Further toward the extracellular side, the flexible guanidinium side chain of Arg^{72} points away from the Schiff base and toward the extracellular side, as in archaeal sensory rhodopsin II (*7*); however, here Arg^{72} is flanked by two histidines (His^{69} and His^{8}).

Comparison of the cytoplasmic half of *Anabaena* sensory rhodopsin with those of other microbial rhodopsins reveals markedly increased hydrophilicity in this region (Fig. 2B). The active site near the middle of the bilayer is connected to the cytoplasm via a hydrophilic path that contains at least four water molecules. A number of hydrophilic side chains interact with these water molecules to form an almost continuous hydrogen-bonded network from the Lys^{210} carbonyl to the cytoplasm over a distance of 19 Å: Lys^{210} – Wat^{502} – Ser^{214} – Asp^{217} of helix G; Ser^{86}, Thr^{90}, and Gln^{93} of helix C and the C-D loop; and Glu^{36} of helix B (Fig. 2B). In contrast, the cytoplasmic region of the haloarchaeal sensory rhodopsin II is entirely hydrophobic (*7*). Most notably, Phe^{86} in the archaeal protein occupies the space occupied by three water molecules and Ser^{86} in the center of the hydrophilic path of the *Anabaena* protein. This difference is consistent with the fundamentally different transducer interactions of

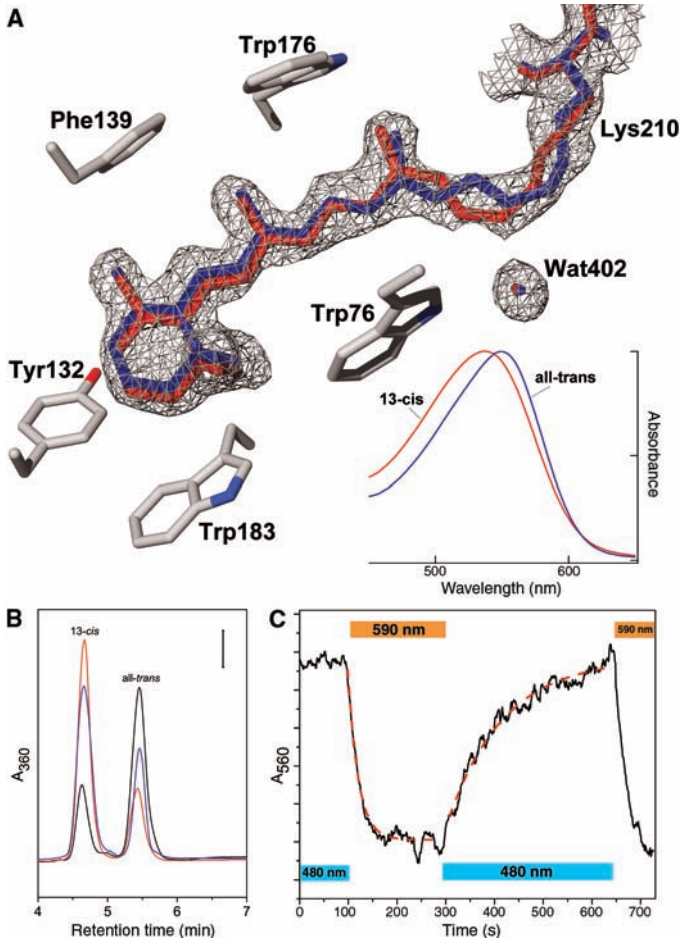

Fig. 1. The electron densities indicate a mixture of retinal isomers. (**A**) Annealed electron density omit map contoured at 1σ with 13-cis,15-syn (in red) and all-trans,15-anti (in blue) retinal models. The density suggests a mixture of all-trans,15-anti and 13-cis,15-syn retinal after white-light illumination (*13*). The conjugated π system of the retinylidene is more bent than in archaeal sensory rhodopsin II, with the distance from the Schiff base nitrogen to the β-ionone C1 reduced to 11.6 Å from 12.2 Å. The increased bent also causes an increase, by 0.6 Å, in the distance between the two tryptophan side chains (Trp^{76} and Trp^{176}) that sandwich the retinal in its binding site. (Inset) Absorption spectra of the 13-cis and trans forms of the pigment calculated from the measured spectra of the orange-illuminated and dark-adapted states using the isomer ratios depicted in (**B**). (**B**) Extraction of retinal isomers from orange-illuminated (580 ± 5 nm, 5 min, red line), blue-illuminated (480 ± 5 nm, 5 min, blue line), and dark-adapted (black line) pigments in detergent-solubilized (0.1% dodecylmaltoside) *Escherichia coli* membranes revealed a decrease of the fraction of 13-cis,15-syn retinal from 82% (orange) to 24% (dark). The units of the A_{360} axis (absorbance at 360 nm) are 2.0×10^{-3}, 1.2×10^{-3}, and 1.2×10^{-3} absorption units for the orange-illuminated, blue-illuminated, and dark-adapted samples, respectively. (**C**) Photoconversion between cis- and trans-forms under continuous monochromatic illumination. Absorbance at 560 nm, greater in the all-trans form compared to the 13-cis form, is used to monitor the wavelength-sensitive spectral transitions. The photoconversions follow approximately first-order kinetics as shown by the single exponential fits (dashed red curves) to the transitions during illumination through 10-nm band-pass interference filters centered at 590 nm or 480 nm, as indicated.

the *Anabaena* photoreceptor (soluble transducer) and haloarchaeal photoreceptor (membrane-embedded transducer) (*2*). For the latter, the cubic lipid phase crystal structure was used to predict the membrane-embedded surface of transducer interaction (*7*), later confirmed by the crystal structure of the receptor bound to a transducer fragment (*9*). The soluble *Anabaena* transducer (*2*) is thought to interact through the receptor's cytoplasmic surface. In the *Anabaena* photosensor, this surface is highly ordered, and all three loops that connect the transmembrane α helices (the A-B, C-D, and E-F loops) are structurally well defined, with conformations substantially different from those of bacteriorhodopsin and sensory rhodopsin II (Fig. 2C). Specifically, Gln^{93} is part of a four-residue insertion in the C-D loop relative to the archaeal receptor that results in an enlarged yet well-ordered cytoplasmic loop near the end of the hydrophilic path, a region likely to interact with the transducer.

As with most other membrane protein crystals prepared from the cubic lipid phase, long, tubular electron densities could be interpreted as lipid tails that form ordered, stacked bilayers in the crystal. Judging from the 13 lipid tails that could be built into electron density, it appears that, in contrast to earlier studies of cubic lipid phase crystals, this bilayer is not planar in *Anabaena* sensory rhodopsin crystals but rather undulates as a result of specific protein-protein interactions within and between bilayers (fig. S1).

The data shown here reveal two photochromic states of *Anabaena* sensory rhodopsin determined by the color of ambient light. The physiological function of the receptor is not yet known, but in cyanobacteria several physiological processes depend on light in the region of its absorption (*2*). For example, cyanobacteria adjust the pigment composition of their photosynthetic light-harvesting complexes based on the color of available light, a phenomenon called chromatic adaptation. Action spectra for chromatic adaptation show that orange light stimulates synthesis of phycocyanin, whereas shorter wavelength blue-green light activates synthesis of phycoerythrin (*21–23*). This color-sensitive pigment synthesis is generally assumed to be based on participation of two competitive receptor pigments with orange versus blue-green absorption maxima. However, the photochromic property of the *Anabaena* pigment shows that it is possible that such color sensing could be achieved by a single photoreceptor, namely the pigment in its two photo-interconvertible groundstates. The signaling mechanism could make use either of the ratio of the two stable groundstate forms or photochemical reaction of one of the forms, because in both cases the photointerconversion between the cis- and trans-forms of the pigment depends on the light quality.

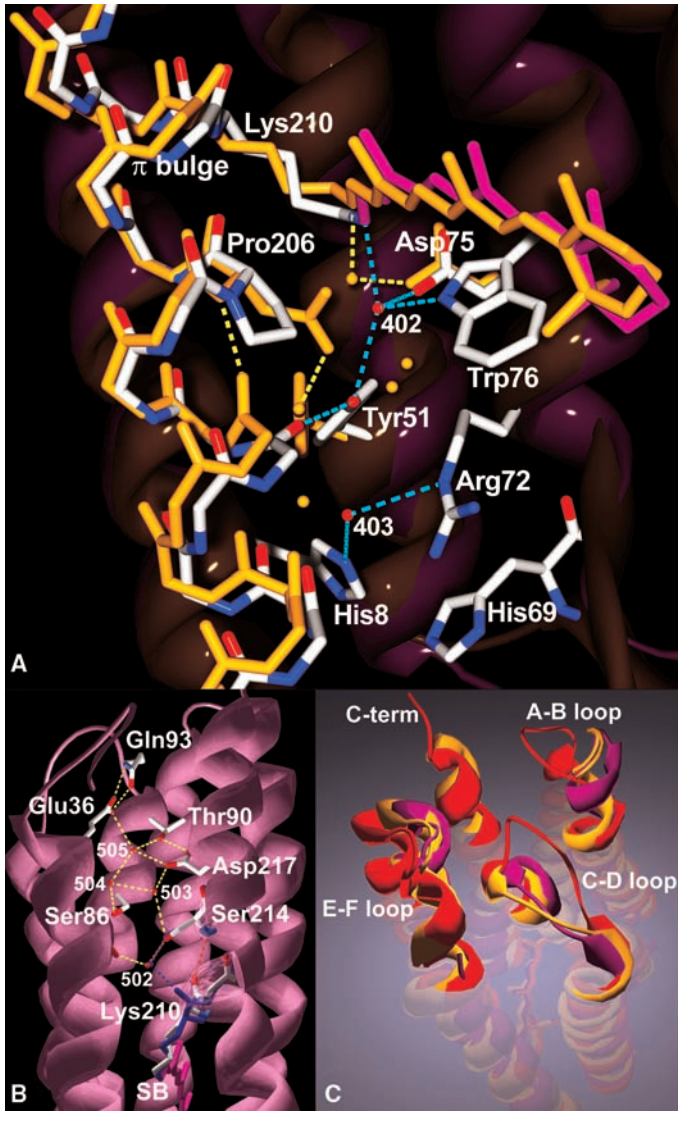

Fig. 2. Structural differences with archaeal rhodopsins. (**A**) The extracellular half of *Anabaena* sensory rhodopsin is shown as purple ribbon with CPK-colored atoms, magenta retinal near the top right, red water molecules, and turquoise hydrogen bonds, with residue numbering according to its sequence. The extracellular surface is near the bottom. The largest differences appear around the Asp-to-Pro mutation at position 206. For comparison, archaeal sensory rhodopsin II is shown in orange throughout with yellow hydrogen bonds. (**B**) The cytoplasmic half of the protein is markedly more hydrophilic than those of other microbial rhodopsins. The cytoplasmic surface is located at the top of the image and the retinal near the bottom. The peptide plane between residues 210 and 211 displays two alternate conformations. In one, Lys^{210} C=O accepts a regular intrahelical hydrogen bond from residue 214 N-H (Lys^{210} shown in blue; hydrogen bonds are shown as red dashed lines). In the other, it accepts a hydrogen bond from Wat^{502} (hydrogen bonds are shown as blue dashed lines). This alternate conformation results in an ~55° change in the orientation of the 210 peptide bond C=O vector, with a movement of the Lys^{210} carbonyl oxygen by 1.8 Å. Only the latter conformation completes a hydrogen bond chain that leads from Lys^{210} C=O at the active site via Wat^{502}, Ser^{214}, OH, and three more ordered waters (Wat^{503}, Wat^{504}, and Wat^{505}) held in place by the side chains of Asp^{217}, Ser^{86} (two alternate side-chain conformations, only one of which is shown for clarity), and Thr^{90} to the cytoplasmic surface near Glu^{36} of helix B and Gln^{93} in the C-D loop. (**C**) A comparison of the loop structures that define the respective cytoplasmic surfaces reveals large differences between the surfaces of archaeal sensory rhodopsin II (orange) and bacteriorhodopsin (purple) and the surface of *Anabaena* sensory rhodopsin (red), which is thought to interact with its soluble transducer. In particular, the A-B and C-D loops of the *Anabaena* protein are packed entirely differently, with relative backbone movements of 10 Å and 7 Å, respectively. The C-D loop contains surface-exposed Phe^{94}/Ile^{95}, Lys^{96}/Lys^{97}, and Trp^{99} side chains, and because of a four-residue insertion relative to sensory rhodopsin II, the loop protrudes 6 Å further into the cytoplasmic space.

References and Notes

1. These pigments, also known as type 1 rhodopsins, are found in each of the three domains of life (i.e., Archaea, Bacteria, and Eucarya), including haloarchaea, proteobacteria, cyanobacteria such as *Anabaena*, fungi, and algae (*2–4*, *24*).
2. K. H. Jung, V. D. Trivedi, J. L. Spudich, *Mol. Microbiol.* **47**, 1513 (2003).
3. O. Béjà *et al.*, *Science* **289**, 1902 (2000).
4. O. A. Sineshchekov, K. H. Jung, J. L. Spudich, *Proc. Natl. Acad. Sci. U.S.A.* **99**, 8689 (2002).
5. H. Luecke, B. Schobert, H. T. Richter, J. P. Cartailler, J. K. Lanyi, *J. Mol. Biol.* **291**, 899 (1999).
6. M. Kolbe, H. Besir, L. O. Essen, D. Oesterhelt, *Science* **288**, 1390 (2000).
7. H. Luecke, B. Schobert, J. K. Lanyi, E. N. Spudich, J. L. Spudich, *Science* **293**, 1499 (2001).
8. A. Royant *et al.*, *Proc. Natl. Acad. Sci. U.S.A.* **98**, 10131 (2001).
9. V. I. Gordeliy *et al.*, *Nature* **419**, 484 (2002).
10. J. C. Venter *et al.*, *Science* **304**, 66 (2004).
11. J. L. Spudich, K. H. Jung, in *Handbook of Photosensory Receptors*, W. Briggs, J. L. Spudich, Eds. (Wiley, Weinheim, Germany), in press.

12. O. A. Sineshchekov, J. L. Spudich, *Photochem. Photobiol. Sci.* **3**, 548 (2004).
13. The traditional notion of light and dark adaptation of microbial rhodopsins (LA and DA, illumination with intense white light and relaxation to thermodynamic equilibrium in the dark, respectively) stems from decades of research on bacteriorhodopsin. For wild-type bacteriorhodopsin, LA produces nearly 100% all-trans retinal, whereas DA yields ~40% all-trans and 60% 13-cis,15-syn retinal. Because for *Anabaena* sensory rhodopsin, neither LA nor DA may represent a physiologically relevant state, we prefer to refer to orange-illuminated or blue-illuminated chromophores. The former encompasses cases in which the incident light is within the pigment's absorption range but of substantially longer wavelength than the λ_{max} of the chromophore and the latter cases where the light is of substantially shorter wavelength.
14. Sensory rhodopsin I produces an attractant signal in response to orange-light–induced trans-to-cis isomerization, and its photocycle contains a transient 13-cis blue-shifted photointermediate. This intermediate's cis-to-trans photoreaction from near-ultraviolet (UV) light generates a repellent signal (*25*). Sensory rhodopsin I therefore detects the presence of near-UV light in an orange-light background over the few seconds' duration of its photocycle. *Anabaena* sensory rhodopsin, in contrast, exhibits two distinct dark groundstate spectral species, each of which is stable for several orders of magnitude longer than their flash-induced photocycles (*26*).
15. Phytochromes exhibit red-absorbing and far-red–absorbing forms that control a variety of phenomena in plants, such as flowering and circadian rhythms. As described for *Anabaena* sensory rhodopsin here, the two forms of phytochrome are each stable in the dark over long periods and are rapidly photointerconverted, properties that provide color-sensitive physiological responses (*16*, *17*, *27*).
16. H. Wang, X. W. Deng, in *The Arabidopsis Book*, C. R. Somerville, E. M. Meyerowitz, Eds. (American Society of Plant Biologists, Rockville, MD, 2002), pp. 1–28.
17. P. Gyula, E. Schäfer, F. Nagy, *Curr. Opin. Plant Biol.* **6**, 446 (2003).
18. W. Gärtner, in *Handbook of Biological Physics*, D. G. Stavenga, W. J. de Grip, E. N. Pugh Jr., Eds. (Elsevier, Amsterdam, 2000), vol. 3, pp. 297–388.
19. J. P. Cartailler, H. Luecke, *Structure* **12**, 133 (2004).
20. H. Luecke, H. T. Richter, J. K. Lanyi, *Science* **280**, 1934 (1998).
21. R. MacColl, *J. Struct. Biol.* **124**, 311 (1998).
22. A. R. Grossman, D. Bhaya, Q. He, *J. Biol. Chem.* **276**, 11449 (2001).
23. B. Singh, V. S. Chauhan, S. Singh, P. S. Bisen, *Curr. Microbiol.* **43**, 265 (2001).
24. J. L. Spudich, C. S. Yang, K. H. Jung, E. N. Spudich, *Annu. Rev. Cell Dev. Biol.* **16**, 365 (2000).
25. J. L. Spudich, R. A. Bogomolni, *Nature* **312**, 509 (1984).
26. O. A. Sineshchekov *et al.*, in preparation.
27. G. Wagner, in *ESP Review Series on Photobiology*, D.-P. Häder, M. Lebert, Eds. (Elsevier, Amsterdam, 2001), pp. 421–448.
28. Supported by NIH grant nos. R01-GM59970 (H.L.), R01-GM067808 (H.L.) and R37-GM27750 (J.L.S.); NSF grant no. 0091287 (J.L.S.); a Welch Investigator Award (J.L.S.); and a Bessel Award from the Alexander-von-Humboldt Foundation (H.L.). The atomic coordinates and structure factors of *Anabaena* sensory rhodopsin are available at the Protein Data Bank with code 1XIO.

Supporting Online Material
www.sciencemag.org/cgi/content/full/1103943/DC1
Materials and Methods
Fig. S1
Table S1
References and Notes

11 August 2004; accepted 22 September 2004
Published online 30 September 2004;
10.1126/science.1103943
Include this information when citing this paper.